Earth Planet. Sci. Lett. 652 (2025) 119200

Contents lists available at ScienceDirect

Earth and Planetary Science Letters

journal homepage: www.elsevier.com/locate/epsl

On the possibility of exhaustive carbonation in geological carbon storage

Jun Korenaga

Department of Earth and Planetary Sciences, Yale University, P.O. Box 208109, New Haven, CT 06520-8109, USA

ARTICLE INFO

Editor: C. Lithgow-Bertelloni

Keywords:
Carbon sequestration
Crystallization pressure
Reaction-driven cracking

ABSTRACT

As a means of geological carbon sequestration, in-situ mineral carbonation has enormous potential, owing to the sheer magnitude of potentially accessible mafic and ultramafic reservoirs. Because carbonation is a solid-volume-increasing reaction, however, the effective exploitation of such subsurface reservoirs depends critically on the efficacy of reaction-driven cracking, which in turn rests on still elusive estimates of crystallization pressure in geological materials. Here we show that, by relating porosity generation with carbonation reaction through elastic strain energy, the maximum degree of in-situ carbonation in the limit of zero crystallization pressure can be expressed as a simple function of the confining pressure, the tensile strength of rocks, the initial porosity, and the relative solid-volume change. This theoretical estimate will help us better interpret laboratory experiments and integrate them with field-scale studies to assess the storage potential of various geological reservoirs under different conditions.

1. Introduction

Among the six major approaches to CO_2 removal and sequestration discussed in the 2019 National Academies report on negative emissions technologies (National Academies of Sciences, Engineering, and Medicine, 2019), carbon mineralization, in particular, in situ carbon mineralization, stands out for its vast potential whereas its 'safe' potential rate of CO_2 removal is, given current technology and understanding, labeled as "unknown". Carbon mineralization refers to accelerated chemical weathering, in which CO_2 from the atmosphere is sequestered into carbonate minerals as a result of aqueous (carbonic acid) reactions with certain silicate rocks such as basalt and peridotite. Resulting carbonate minerals are thermodynamically stable at the Earth's surface and near-surface conditions, allowing practically permanent carbon sequestration. This is in contrast to other means of geologic sequestration such as injecting captured CO_2 into a saline aquifer, the long-term stability of which cannot be guaranteed (Wilson et al., 2003; Rochelle et al., 2024; Zoback and Gorelick, 2012; Bielicki et al., 2014). A representative carbonate forming reaction is Mg_2SiO_4 (forsterite) + 2 CO_2 = 2 $MgCO_3$ (magnesite) + SiO_2 (quartz), so one mole of Mg can take up one mole of CO_2. Based on the amount of carbonate minerals naturally sequestered in geothermal areas in Iceland (Wiese et al., 2008), it has been suggested that basaltic lavas in the global mid-ocean ridge system might have the mineral CO_2 storage capacity of $1-2.5\times10^5$ Gt CO_2 (Snaebjornsdottir et al., 2014). Compared to basalt, peridotite is more enriched in divalent cations that can react with CO_2, and the amount of accessible (in the upper 7 km of the solid Earth) peridotite on continents ($\sim10^{17}$ to 10^{18} kg) and beneath the seafloor ($\sim10^{20}$ kg) translates to the maximum sequestration of 4×10^4 to 4×10^7 Gt CO_2 (Kelemen et al., 2011). As the current global CO_2 emissions are ~50 Gt yr^{-1}, carbon mineralization appears to be extremely promising. For comparison, the safe potential rate of CO_2 removal at a price of less than \$100/t CO_2 is estimated to be at, on a global scale, 0.13 Gt yr^{-1} for coastal blue carbon, 1 Gt yr^{-1} for afforestation and reforestation, 1.5 Gt yr^{-1} for forest management, 1.5 Gt yr^{-1} for enhanced soil carbon storage, and 3.5-5.2 Gt yr^{-1} for bioenergy with carbon capture and sequestration (BECCS) (National Academies of Sciences, Engineering, and Medicine, 2019). Among these, BECCS comes with the highest potential rate, but it involves carbon sequestration, in which in situ carbon mineralization may play a role.

Calculations of the storage potential of such basaltic and peridotitic reservoirs vary substantially with what assumptions are adopted. One end-member approach is to consider just the porosity of rocks as space to store carbonated water or supercritical CO_2 (i.e., mineralization serves only as a safeguard for potential leakage) (McGrail et al., 2006; Goldberg et al., 2008; Marieni et al., 2013). The other end-member is to assume that all MgO and CaO components of rocks are available for mineralization (FeO would be available for carbonation only under reducing conditions) (Kelemen and Matter, 2008; Kelemen et al., 2011). For example, 1 m^3 of typical basaltic rock (8 wt% MgO, 10 wt% CaO, and a density of 3000 kg m^3) with 10% porosity would store ~6 kg CO_2 with carbonated water or ~20 kg CO_2 with supercritical CO_2 (assuming 40 °C and 7.5 MPa), but it could store as much as ~450 kg CO_2 if

E-mail address: jun.korenaga@yale.edu.

https://doi.org/10.1016/j.epsl.2024.119200
Received 27 August 2024; Received in revised form 8 December 2024; Accepted 31 December 2024

all MgO and CaO are used for carbonation. As developing geological sequestration sites involves various scientific, engineering, financial, and legal concerns, an accurate estimate of a realistic storage potential is essential when evaluating and prioritizing different site candidates. In this regard, it is important to understand the plausibility of exhaustive reaction of divalent cations (i.e., Mg^{2+} and Ca^{2+}) in rocks, as it corresponds to the highest estimate of storage potential.

A well-recognized hurdle for such an exhaustive reaction is that carbonation reactions, being all solid-volume-increasing, may quickly clog the pore space and thus be self-limiting. At the same time, volume-increasing reactions may generate enough stresses to crack ambient rocks and create new pore space, as suggested by field observations (Jamtveit et al., 2008; Kelemen and Matter, 2008; Kelemen and Hirth, 2012), theoretical considerations (Fletcher et al., 2006; Rudge et al., 2010; Ulven et al., 2014; Evans et al., 2020), and laboratory experiments (Zhu et al., 2016; Zheng et al., 2018; Lambert et al., 2018; Uno et al., 2022). In particular, the existence of listwanites—rocks composed of Mg-rich carbonates, quartz, and chromian spinel, formed by complete carbonation of all MgO and CaO initially in mantle peridotite—demonstrates that complete carbonation is attainable under some geological conditions (Kelemen et al., 2011). It is still unclear, however, whether such exhaustive reaction of divalent cations can be achieved under the conditions achievable by engineering. All known listwanites in Oman, for example, are likely to have formed as a result of the metamorphic dehydration of the CO_2-bearing sediments that were overthrusted by hot peridotite (Kelemen et al., 2011).

One major concern is that crystallization pressure (or force of crystallization), which is instrumental in most of the proposed mechanisms for reaction-driven cracking, may not be as high as theoretically predicted. For example, the hydration of periclase has an expected crystallization pressure of ∼1.9 GPa, but experimental results indicate less than 2% of the theoretical magnitude (Zheng et al., 2018). In light of the existing uncertainty about the realistic magnitude of crystallization pressure, one practical way forward is to constrain the minimum extent of reaction-driven cracking using elastic strain energy only (Fletcher et al., 2006). This alternative theoretical formulation allows us to derive a simple theoretical prediction for the extent of a solid-volume-increasing reaction and to define the critical depth, above which the exhaustive reaction of divalent cations is possible even without invoking crystallization pressure. The theoretical framework presented in this study also helps to reevaluate the previous experimental efforts on quantifying crystallization pressure. In what follows, we will first review the major unresolved issues of crystallization pressure in the context of its geological application. We will then present our theoretical framework that is solely based on elastic strain energy, with some sample applications. We will close by discussing the implications of our theory for published experimental results as well as geological carbon sequestration.

2. Volume-increasing reaction and crystallization pressure

Crystallization pressure refers to the pressure exerted by a confined crystal that continues to grow against a constraint, and there have been numerous experimental and theoretical studies since its first discovery in the mid-19th century (e.g., Scherer, 1999; Steiger, 2005). For a crystal to grow toward its constraint, there must exist a supersaturated solution film between the crystal's loaded face and the constraint; a substance needed for crystal growth cannot be delivered otherwise. As the solubility of crystals generally increases with pressure, a crystal can potentially grow until the pressure in such a solution film becomes so high that the solution becomes no longer supersaturated. For such a solution film to exist, however, there must be repulsion (called disjoining pressure) between the growing crystal and the constraint, so crystal growth would stop when crystallization pressure exceeds disjoining pressure. The classical situation under which crystallization pressure has been studied is direct precipitation from a typically stoichiometrically supersaturated solution, but its thermodynamic framework has been extended for more complex chemical reactions appropriate for the hydration and carbonation of geological materials (Kelemen et al., 2011; Kelemen and Hirth, 2012; Wolterbeek et al., 2018). According to these studies, the serpentinization and carbonation of olivine can exert crystallization pressure on the order of a few hundred MPa to >1 GPa (Kelemen and Hirth, 2012), and the hydration of CaO can exert crystallization pressure of a few GPa (Wolterbeek et al., 2018). As lithostatic pressure within Earth's crust is ∼30 MPa and ∼300 MPa, respectively, at a depth of 1 and 10 km, the potential of crystallization pressure to facilitate subsurface reaction-driven cracking is clear.

Such theoretical predictions of high crystallization pressure are, however, yet to be verified by experiments. As noted earlier, the hydration of periclase (MgO) to create brucite ($Mg(OH)_2$) is predicted to have crystallization pressure of ∼1.9 GPa at 200 °C, but the experiments conducted under this temperature condition showed that reaction-driven cracking virtually ceased with the confining pressure (the difference between solid and fluid pressures) greater than 30 MPa (Zheng et al., 2018). The authors of this experimental study suggested that disjoining pressure in the periclase-brucite system might be only ∼30 MPa, which acted as a bottleneck. Disjoining pressure plays a fundamental role in the wetting of a solid surface with a liquid film, and the physics of such a thin liquid film, which is usually only a few nanometer thick, is not well understood, as it can be dictated by microscopic details such as interaction energy and roughness (Li et al., 2022). Alternatively, it is suggested that crystallization pressure in these experiments may be limited by the low frictional yielding of brucite (Kelemen et al., 2018). Because nearly complete reaction was achieved at lower confining pressures (Zheng et al., 2018), this explanation would work if the cohesive strength, which is pressure-independent, of brucite in their samples is ∼30 MPa. The friction coefficient of brucite gouge has been estimated to be ∼0.45 (Moore and Lockner, 2004, 2007), but its cohesive strength is assumed to be zero in these measurements. In general, the measurements of cohesive strengths depend on the conditions of sampled used (Lockner, 1995), and a low friction coefficient does not necessarily indicate a low cohesive strength. Serpentinized peridotites, for example, have low friction coefficients, but there is no appreciable reduction in cohesive strength, which is ∼100 MPa (Escartin et al., 2001).

Similar discrepancy between a theoretical estimate and experimental observations is seen for the hydration of CaO to $Ca(OH)_2$ (Wolterbeek et al., 2018; Lambert et al., 2018), for which crystallization pressure is predicted to be as high as >3 GPa. The solid volume increase for this reaction is 96%, and the sample volume expansion was observed up to the confining pressure of ∼150 MPa in the experiments of Wolterbeek et al. (2018). At a higher pressure (225 MPa), negative changes in the sample volume were observed instead. In the experiments of Lambert et al. (2018), the maximum confining pressure tested is ∼27 MPa, at which a positive change in the sample volume was still observed. In both experiments, a change in the sample volume decreases monotonically with the confining pressure. In addition to low crystallization pressures compared to what is theoretically predicted, this pressure dependence is not easy to explain with the thermodynamics of crystallization pressure. For a given chemical reaction, crystallization pressure is primarily a function of temperature, so its effect would not lessen with increasing pressure until the confining pressure reaches crystallization pressure or disjoining pressure. Wolterbeek et al. (2018) attributed the observed pressure dependence to the effect of pressure on sample permeability; permeability may have been reduced at higher pressure, thereby lowering the efficiency of hydration reaction. However, the time-series data of sample volume change reported by Lambert et al. (2018) show that this pressure dependence is observed even from the beginning of their experiments, at which the sample porosities were likely close to their initial high values (40-50%).

3. Reaction-driven cracking with elastic strain energy

With the notion of crystallization pressure, full chemical reaction is theoretically possible when confining pressure is lower than crystallization pressure (or disjoining pressure if the latter is lower). Of course, such a full reaction may not be achieved owing to various realistic complications such as the reduction of permeability by compaction and the armoring of reactive surfaces with product phases. Nevertheless, crystallization pressure offers a simple theoretical upper bound for in situ mineral carbonation. If crystallization pressure for carbonation is 300 MPa (Kelemen and Hirth, 2012), for example, efficient carbonation is expected down to the depth of ∼10 km. However, given the existing uncertainties pertinent to the crystallization pressures of geological materials as discussed in the previous section, it would be beneficial to explore the effect of confining pressure on volume-increasing chemical reactions, in the limit of zero crystallization pressure. In fact, such theoretical exploration is relatively straightforward with the use of elastic strain energy, as shown in the following.

Our theoretical formulation is intended to be parsimonious, with most of realistic complications encapsulated in two efficiency factors (f_1 and f_2). For example, we do not consider, at least explicitly, the effect of permeability, the efficiency of solute transport, the effect of porosity on tensile strength, and so on. All of these complications simply lower the likelihood of exhaustive carbonation, thereby increasing the graveness of the theoretical upper bound indicated by our theory.

3.1. Theoretical formulation

Consider the chemical reaction taking place in a homogeneous porous medium located at a depth of z:

$$A + W \rightarrow B, \tag{1}$$

where A represents unreacted solid components collectively, W represents a fluid phase (e.g., water with or without some dissolved components such as CO_2), and B represents reacted solid components collectively. The relative change in the solid volume after the reaction is denoted as $\Delta V_s/V_s$ ($=(V_B - V_A)/V_A$). To simplify the notation, the above phases A and B can contain unreactive components (i.e., it also includes a reaction like $A + C + W \rightarrow B + C$), and the presence of such unreactive components in the system reduces the effective volume change. The temporal evolution of porosity, ϕ, and the fractions of the phases A and B, ϕ_A and ϕ_B, respectively, may be described by

$$\frac{\partial \phi}{\partial t} = -R, \tag{2}$$

$$\frac{\partial \phi_A}{\partial t} = -R\frac{\Delta V_s}{V_s}, \tag{3}$$

$$\frac{\partial \phi_B}{\partial t} = R\left(1 + \frac{\Delta V_s}{V_s}\right). \tag{4}$$

Here R is the reaction rate defined as

$$R = \alpha_s v_r \frac{\phi_A}{\phi_A + \phi_B}, \tag{5}$$

where α_s is the specific surface area density, which may be calculated as $2\phi/w$ with w being the width of void opening, and v_r is the speed at which reaction propagates. This formulation of the reaction rate guarantees that the phase A, as long as it exists, is always available for reaction in its relative proportion. Given the likely armoring of reactive surfaces by reaction products, this formulation corresponds to the maximum reaction rate. The initial condition is set as $\phi(0) = \phi_0$, $\phi_A(0) = 1 - \phi_0$, and $\phi_B(0) = 0$, and the following conservation of volume holds at all time:

$$\phi + \phi_A + \phi_B = 1. \tag{6}$$

The relative change in the solid volume can also lead to the linear elastic strain, ϵ, as

$$\frac{\partial \epsilon}{\partial t} = f_1 \frac{R}{3}\left|\frac{\Delta V_s}{V_s}\right|, \tag{7}$$

where f_1 denotes the fraction of the system volume change contributing to the linear elastic strain. With a free-moving fluid phase, a change in the solid volume does not necessarily result in elastic strain, so f_1 can be lower than unity. Assuming f_1 of 1 corresponds to zero eigenstrain (Mura, 1987). The strain starts at zero at $t = 0$, and it can continue to grow until it reaches the maximum strain ($\epsilon_{\max}$), which is determined by the tensile strength (σ_T) and Young's modulus (E) of the rocks under consideration as

$$\epsilon_{\max} = \frac{\sigma_T}{E}. \tag{8}$$

When the linear strain exceeds it maximum value, the accumulated elastic energy will be released by fracturing, which can create a new porosity, and the linear elastic strain is reset to zero. An increase in porosity, $\Delta\phi$, and the elastic energy must be related as

$$\Delta\phi P_{\text{conf}} = f_2 \frac{E\epsilon_{\max}^2}{1-\nu}, \tag{9}$$

where f_2 denotes the fraction of elastic energy density used for increasing porosity and ν is the Poisson ratio of the rocks. The left-hand side of the above equation represents the energy density required to increase the porosity by $\Delta\phi$ under the confining pressure, P_{conf}. The factor f_2 can be lower than unity because part of elastic strain energy may be used to generate new surfaces (Fletcher et al., 2006) or adjust the pore geometry. Viscoelastic relaxation is, however, deemed unlikely because the viscosity of the rock matrix should be sufficiently high at shallow geological reservoirs where temperatures do not exceed a few hundred °C.

The confining pressure increases with depth as

$$P_{\text{conf}} = \Delta\rho g z, \tag{10}$$

where $\Delta\rho$ is the density difference between the rocks and water and g is gravitational acceleration. This assumes that the pore fluid is at the hydrostatic pressure, which is appropriate for the open aquifer setting required for continuous fluid injection (Zhou et al., 2008; Thibeau et al., 2014). In the closed aquifer setting, the pore fluid pressure could reach lithostatic, nullifying the confining pressure, but in this case, the degree of maximum reaction is simply determined by the volume of the pre-existing pore fluid. When the porosity is increased by $\Delta\phi$ at time t, ϕ_A and ϕ_B are multiplied by the factor $(1 - \phi(t^+))/(1 - \phi(t^-))$, where $\phi(t^+) = \phi(t^-) + \Delta\phi$, to maintain mass balance (equation (6)). This can be interpreted to result from the expansion of the relevant system volume (see equation (18)).

As can be inferred from equations (9) and (10), creating new porosity is more difficult at greater depths. If the initial porosity has no depth variation, we may define the critical depth, z_c, as the depth below which the complete reaction of the phase A is impossible. At the critical depth, the following energy balance holds:

$$\left(\phi_A(0)\frac{\Delta V_s}{V_s} - \phi(0)\right)\Delta\rho g z_c = f_2 \frac{E\epsilon_{\max}^2}{1-\nu}\left(\frac{\epsilon_{\text{total}}}{\epsilon_{\max}}\right), \tag{11}$$

where the left-hand side represents the energy density required to create a new porosity to compensate for the solid volume increase by full reaction and the right-hand side is available elastic energy density produced during such a full reaction. Because the total linear elastic strain, ϵ_{total}, is given as

$$\epsilon_{\text{total}} = \frac{f_1}{3}\phi_A(0)\left|\frac{\Delta V_s}{V_s}\right|, \tag{12}$$

equation (11) may be solved for the critical depth as

$$z_c = \frac{f_1 f_2}{3}\frac{\sigma_T}{\Delta\rho g(1-\nu)}\left(1 - \frac{\phi(0)}{\phi_A(0)}\frac{V_s}{\Delta V_s}\right)^{-1}. \tag{13}$$

Equation (13) is valid only when $\phi(0) < \phi_A(0)\Delta V_s/V_s$, that is, when the creation of new porosity is required for full reaction. With a sufficiently high initial porosity ($\phi(0) \geq \phi_A(0)\Delta V_s/V_s$), full reaction is possible regardless of depth.

Below the critical depth, the maximum degree of reaction may be given as a function of confining pressure:

$$\xi_{\max} \equiv 1 - \frac{\phi_A(\infty)}{\phi_A(0))} = \frac{\phi(0)}{\phi_A(0)} \frac{V_s}{\Delta V_s} \left(1 - \frac{f_1 f_2 \sigma_T}{3(1-\nu)P_{\text{conf}}}\right)^{-1}, \tag{14}$$

which converges to $\phi(0)V_s/(\phi_A(0)\Delta V_s)$ as $\sigma_T \to 0$ or $P_{\text{conf}} \to \infty$. Note that equations (13) and (14) are only approximate because the creation of new porosity during the process under consideration prevents equations (11) and (12) to be exact.

The critical depth is defined as the depth below which complete reaction is impossible, but new porosity generation by the release of elastic strain energy is still possible below the critical depth. To better illustrate the effect of confining pressure, therefore, it is convenient to introduce the critical depth of the second kind, below which new porosity generation becomes negligible. Because the number of crack opening is approximately $\epsilon_{\text{tot}}/\epsilon_{\max}$, the total porosity generation may be expressed as

$$\Delta\phi_{\text{tot}} = \frac{f_1 f_2 \sigma_T}{3P_{\text{conf}}(1-\nu)} \phi_A(0)\xi_{\max} \left|\frac{\Delta V_s}{V_s}\right|. \tag{15}$$

Below the critical depth ($\xi_{\max} < 1$), by using equation (14), the above expression reduces to

$$\Delta\phi_{\text{tot}} = \phi(0) \left(\frac{3P_{\text{conf}}(1-\nu)}{f_1 f_2 \sigma_T} - 1\right)^{-1}. \tag{16}$$

In this paper, the second critical depth, z_{c_2}, is defined as the depth below which $\Delta\phi_{\text{tot}} < \Delta\phi_c$, where $\Delta\phi_c$ is set to 0.01. Using equation (16), it may be explicitly written as

$$z_{c_2} = \frac{f_1 f_2}{3} \frac{\sigma_T}{\Delta\rho g(1-\nu)} \left(1 + \frac{\phi(0)}{\Delta\phi_c}\right). \tag{17}$$

Note that the total porosity generation is equivalent to the total expansion of the system volume, i.e.,

$$\left(\frac{\Delta V}{V}\right)_{\text{tot}} = \Delta\phi_{\text{tot}}. \tag{18}$$

3.2. On the magnitude of effective solid-volume expansion

The magnitude of effective solid-volume expansion by carbonation, $\Delta V_s/V_s$, can vary considerably depending on rock composition and fluid chemistry. To derive rough estimates for discussion, however, we assume that all CaO component is consumed by

$$CaSiO_3 + CO_2 \to CaCO_3 + SiO_2, \tag{19}$$

and all MgO component by

$$Mg_2SiO_4 + 2CO_2 \to 2MgCO_3 + SiO_2. \tag{20}$$

The first and second carbonation reactions result in ~46% and ~84% solid-volume expansion, respectively. To calculate the effective solid-volume expansion, we treat the SiO_2, FeO, and Al_2O_3 components as quartz, wüstite, and corundum, respectively, and use their molar volumes. For a basalt composition (50.5 wt% SiO_2, 7.6 wt% MgO, 10.4 wt% FeO, 14.7 wt% Al_2O_3, and 9.4 wt% CaO (Gale et al., 2013)), the effective solid-volume expansion is ~30%, and for a peridotite composition (40.0 wt% SiO_2, 40.9 wt% MgO, 7.3 wt% FeO, and 0.6 wt% CaO (Lippard et al., 1986)), it is ~76%. These values are presented here just to indicate that the solid-volume expansion is on the order of a few 10s of %, and that we expect a greater solid-volume expansion for peridotitic rocks. Other carbonation reactions with different degrees of volume expansion may be thermodynamically favored, in which some of divalent cations are consumed by hydration instead of carbonation. For example, the following reaction (Kelemen et al., 2011),

$$4Mg_2SiO_4 + CaMgSi_2O_6 + CO_2 + 6H_2O \to 3Mg_3Si_2O_5(OH)_4 + CaCO_3, \tag{21}$$

causes a solid-volume expansion of ~40%.

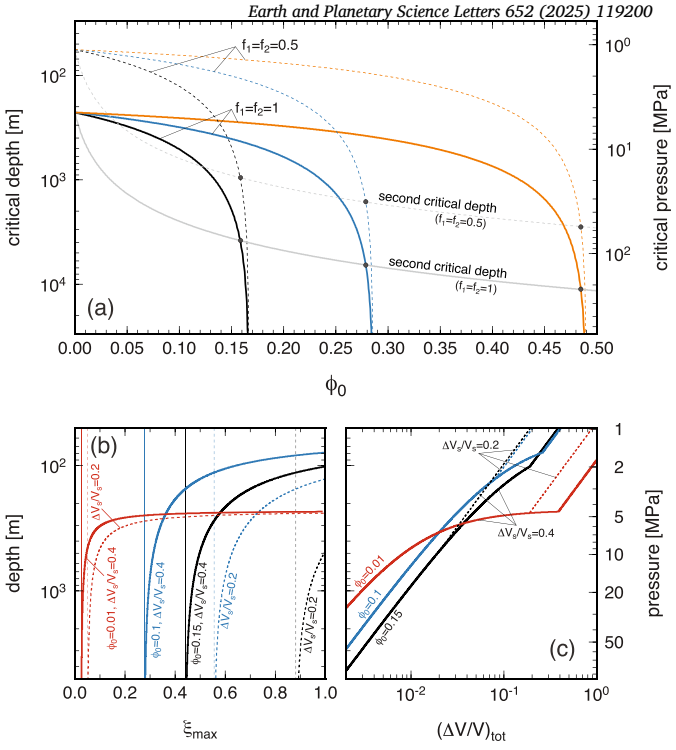

Fig. 1. (a) The critical depth, above which the exhaustive reaction of divalent cations is possible, as a function of initial porosity (ϕ_0), with different values of relative solid-volume change ($\Delta V_s/V_s$ = 0.2 (black), 0.4 (blue), and 0.96 (orange)) and different conversion efficiencies ($f_1 = f_2 = 1$ (solid) and $f_1 = f_2 = 0.5$ (dashed)). Also shown in gray is the second critical depth, below which new porosity generation becomes less than 1%. The corresponding critical pressure is shown to the right. (b) The maximum degree of reaction ($\xi_{\max}$) as a function of depth, for a few representative cases: $\phi_0 = 0.15$ (black), $\phi_0 = 0.1$ (blue), and $\phi_0 = 0.01$ (red). Conversion efficiencies are set to $f_1 = f_2 = 0.5$ for the first two and $f_1 = f_2 = 1$ for the last. Two values of solid-volume change are used: 0.4 (solid) and 0.2 (dotted). Thin vertical lines denote respective limits at $z \to \infty$. (c) The increase in the system volume by new porosity generation, corresponding to the cases shown in (b). Panels (b) and (c) share the same depth and pressure scales.

3.3. Representative results

The critical depth, above which the exhaustive reaction of divalent cations is possible even without crystallization pressure, is controlled primarily by the initial porosity and the relative solid-volume increase by carbonation (Fig. 1a). The critical depth is also affected by the tensile strength and the Poisson ratio of rock matrix and the density difference between the rock matrix and the pore fluid, but their variations are limited. Greater uncertainties come from two efficiency factors, f_1 (the fraction of solid-volume change resulting in elastic strain) and f_2 (the fraction of elastic energy used for porosity generation); we use $f_1 = f_2 = 1$ for maximum critical depths and $f_1 = f_2 = 0.5$ for more realistic estimates. At low initial porosities ($\phi_0 \sim 0$), the maximum critical depth is predicted to be ~230 m for the tensile strength of 10 MPa. A greater critical depth is possible with a greater tensile strength, but available

rock mechanical data suggest that it is unlikely (Cai, 2010; Perras and Diederichs, 2014). The critical depth reduces to only ~100 m with more plausible efficiency factors ($f_1 = f_2 = 0.5$). These shallow depths clearly reflect the influence of confining pressure on porosity generation in the absence of crystallization pressure.

The critical depth is just one measure for the effect of confining pressure, and as it is defined as the depth above which a complete reaction is possible, it may be too strict. This is why we introduced in the above the second critical depth, below which the new porosity generation becomes less than 1%. As seen in Fig. 1a, the second critical depth can be a few times deeper than the first critical depth. Naturally, a greater initial porosity lowers the impact of volume increase by reaction, and the (first) critical depth eventually exceeds the second one and diverges at sufficiently high initial porosities (Fig. 1a), meaning that exhaustive reaction is possible without new porosity generation. The possible extent of carbonation below the critical depth can be assessed by the maximum degree of reaction, which is also controlled primarily by the initial porosity and the relative volume increase by carbonation (Fig. 1b). The maximum degree of reaction converges to a simple limit that can readily be derived from the initial porosity and the relative solid-volume increase, but for sufficiently large initial porosity, the convergence takes place over a few hundred meters to >1 km, allowing substantial reaction even below the critical depth. Shown in Fig. 1c is the system volume changes corresponding to the cases shown in Fig. 1b. The volume change is inversely proportional to confining pressure, and this pressure dependence is linear above the critical depth, and below the critical depth, the dependence remains nearly linear with high initial porosities (Fig. 1c).

The prediction of a higher initial porosity yielding more complete reaction (equation (14)) may appear contradicting the previous studies suggesting that confined crystal growth capable of fracturing rocks is difficult to achieve in high-porosity rocks (e.g., Røyne and Jamtveit, 2015; Heap et al., 2021; Jackson et al., 2024). But this prediction simply stems from the fact that complete reaction is possible, even without any new porosity generation, if an initial porosity is sufficiently high. When reaction-driven cracking is ineffective unless both porosity and pore size are low, this effect can readily be emulated by reducing f_1 and f_2.

4. Discussion and outlook

4.1. Comparison with experimental studies

The critical depth is estimated to be at most ~230 m (equivalent to the confining pressure of ~4.5 MPa) for the tensile strength of 10 MPa, when the initial porosity is small, but it can diverge to infinity if the initial porosity is sufficiently large for a given solid-volume increase (Fig. 1a). This dependence on initial porosity is important when discussing previous experimental efforts on crystallization pressure. For example, the CaO-hydration experiments of Lambert et al. (2018) show nearly complete reaction up to the confining pressure of ~27 MPa, but this observation alone does not automatically support the existence of crystallization pressure. Because the initial porosity of their sample used for the highest confining pressure is as high as ~50%, it is possible to achieve complete reaction down to the confining pressure of ~100 MPa, even without crystallization pressure (Fig. 1a, orange lines). On the other hand, the MgO-hydration experiments of Zheng et al. (2018) show nearly complete reaction up to ~30 MPa even with the low initial porosity (~1%). A more recent experimental study on MgO hydration also shows that a substantial reaction is possible at the confining pressure of 20 MPa even with a very low initial porosity (<0.1%) (Uno et al., 2022). The effect of crystallization pressure seems to be essential to explain these experimental results.

However, it may still be possible to explain these hydration experiments with our theory of elastic strain energy, because the critical depth becomes deeper for higher tensile strength. Experimental studies on volume-increasing reactions typically use sintered samples with small grain size (e.g., <20 μm (Zhu et al., 2016) and 50-80 μm (Uno et al., 2022)), and as the tensile strength is inversely proportional to the square-root of grain size (the Hall-Petch effect (Paterson and Wong, 2005; Scholz, 2019)), the tensile strength can easily be one order of magnitude greater (i.e., ~100 MPa). Sintered synthetic samples are also expected to be stronger than natural rocks. The solid-volume change of MgO hydration is 119%, so if the tensile strength of the samples used by Uno et al. (2022) is >36 MPa, for example, their experimental results are fully consistent with our theory.

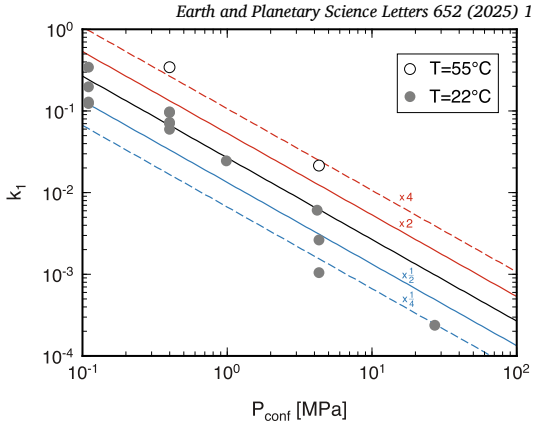

Fig. 2. Relative change in system volume observed at a time of 1 hour in the CaO-hydration experiments of Lambert et al. (2018) (conducted at 22°C (gray circles) and 55 °C (open circles)), compared with the theoretical prediction of porosity generation through elastic strain energy (equation (18)). The following parameters are used for the reference prediction (black line): $f_1 = f_2 = 0.5$, $\nu = 0.25$, $\phi_A(0) = 0.5$, $\sigma_T = 5$ MPa, $\xi = 0.1$, and $\Delta V_s/V_s = 0.96$. The effect of varying the product of $f_1 f_2 \sigma_T \xi$ by a factor of 2 or 4 is shown by colored lines.

Our theory also offers a simple explanation for the pressure dependence of system volume change observed in the CaO-hydration experiments (Wolterbeek et al., 2018; Lambert et al., 2018) (Fig. 2). As mentioned earlier, this pressure dependence is not readily derived from the theory of crystallization pressure. On the other hand, the dependence is expected in our theory because the generation of new porosity is regulated by confining pressure (equation (9)). The time-series data of volume change reported by Lambert et al. (2018) are useful for this kind of comparison with theory. As reaction proceeds, the total porosity generation can become very high (Fig. 1c) at low confining pressures, meaning that a sample porosity can become very high. Naturally, too high porosities are structurally unstable, and a dynamic balance between compaction and new porosity generation is expected to determine the evolution of system volume change. As done in Fig. 2, therefore, comparison between theory and experiments makes sense only for the early phase of experimental runs, where such complications are likely to be minimal.

Our theory is derived in the limit of zero crystallization pressure, but as the above discussion implies, it will also be useful for future experimental efforts on crystallization pressure. First and foremost, it will be important to include the measurement of the tensile strengths of samples. For example, two experimental studies on CaO hydration used similar experimental setups (Wolterbeek et al., 2018; Lambert et al., 2018), but their sample preparations are different. CaO powder was compacted at the pressure of 250 MPa in Wolterbeek et al. (2018) whereas it was done at 24-45 MPa in Lambert et al. (2018), and this difference may have resulted in stronger samples in the former, allowing positive changes in the system volume even at the pressure of 150 MPa. Even without the direct measurement of sample tensile strength, it may be possible to estimate it by conducting experiments at a wide range of initial porosity and confining pressure, as our theory predicts that the critical depth is a simple function of these variables (Fig. 1a). Existing experimental efforts are limited to exploring the effect of pressure with limited variations in initial porosity (Zheng et al., 2018; Wolterbeek et al., 2018; Lambert et al., 2018) or the effect of initial porosity at constant pres-

sure (Uno et al., 2022). It will also be important to better understand the frictional strength of reactants and products, which could limit the efficacy of crystallization pressure (Kelemen et al., 2018).

4.2. Importance of initial porosities

In the absence of crystallization pressure, the restriction imposed by the critical depth is particularly severe when the initial porosity is low (Fig. 1b). With 50% conversion efficiencies from reaction to porosity generation, the critical depth would be less than 60 m (Fig. 1a). Within the framework of our theory, the possibility of exhaustive carbonation at depths thus depends heavily on the preexisting porosity, because porosity generation by hydraulic fracturing is limited. A permeability of 10^{-15} m^2 achieved by hydraulic fracturing (Audigane et al., 2002), for example, corresponds to the porosity of only 10^{-3}, when interpreted with the Blake-Kozeny porosity-permeability relation (Dullien, 1979).

Understanding crystallization pressure in carbonation reaction, therefore, becomes critical to evaluate the sequestration potential of peridotitic reservoirs, which are typically characterized with low porosities (Kelemen et al., 2011). It should also concern the effort to combine the mining of critical minerals such as nickel from peridotite with in-situ carbon mineralization (Nagurney et al., 2023). There are a number of field observations that suggest efficient reaction-driven cracking at substantial depths (Kelemen and Matter, 2008; Kelemen et al., 2011, 2018). However, the geological occurrence of deep hydration or carbonation, e.g., the serpentinization of the forearc mantle (Hyndman and Peacock, 2003), does not necessarily require high crystallization pressure. When fluids are tectonically bought down to great depths such as in the subduction of hydrated oceanic crust and its subsequent dehydration, the fluid pressure would be lithostatic, thereby eliminating the confining pressure. In other words, if the fluid pressure can become as high as lithostatic, our theory predicts that volume-increasing reaction would proceed to its completion even without crystallization pressure. In contrast, fluid injection for in situ carbon mineralization likely requires the open aquifer setting, in which the pore fluid pressure would remain hydrostatic. As noted in the introduction section, the carbon storage potential of peridotitic reservoirs is vast. This underlines the need for further studies to unambiguously quantify the magnitude of crystallization pressure for reactions involving peridotite, and our theory should help the design and interpretation of such experimental efforts.

4.3. Implications for in situ carbon sequestration

In contrast to peridotitic reservoirs, geological reservoirs with high porosities, such as flood basalt provinces, may look more promising. For example, the Columbia River basalt group is estimated to cover the 164,000 km^2 with a total of 100-m-thick, high-porosity (~15%) lava flow tops distributed within the top 1 km (McGrail et al., 2006). The high porosity of the lava flow tops, combined with the relatively low volume increase expected for the carbonation of basaltic rocks (the Columbia River basalt has ~5 wt% MgO and ~9 wt% CaO), indicates the possibility of nearly exhaustive carbonation down to the depth of ~1 km (Fig. 1b). However, the amount of CO_2 that can be dissolved in water is rather low at these depth levels, and CO_2 can be in a supercritical state only below the depth of ~800 m. Thus, the process of CO_2 transport is likely to be the rate-limiting factor that prevents exhaustive carbonation.

The maximum degree of reaction for deep-water basaltic reservoirs is more limited because of high confining pressures, but high confining pressures also allow supercritical CO_2. For example, an area of ~78,000 m^2 around the Juan de Fuca Ridge, within a few hundred kilometers from the northwestern U.S., is covered with >200 m of sediments and located at >2.7 km depth, thus being suitable for structural and gravitational trapping. Utilizing its top 100 m of high-porosity (10%) basaltic layer, it has been suggested that the region can store 780 Gt CO_2 as liquefied CO_2, or 930 Gt CO_2 as carbonate (Goldberg et al., 2008). With 10% initial porosity and 20% relative solid-volume increase, our theory predicts that the maximum degree of reaction is ~0.55 at the limit of $P_{conf} \to \infty$ (Fig. 1b), which translates to 1.5 Tt CO_2. This is ~60% greater than the estimate based on simply filling the porosity with carbonate. As it can be understood from equation (14), taking the limit of $P_{conf} \to \infty$ is equivalent to taking the limit of the product of the efficiency factors ($f_1 f_2$) to zero, i.e., with no generation of new porosity by reaction-driven cracking. This corresponds to the most effective use of the preexisting porosity by carbonation, which has to overcome the likely armoring of reactive surface.

The concept of the critical depth and the maximum degree of reaction will be useful for synergizing laboratory experiments, field-scale experiments, and geological records to better assess the storage potential of different geological reservoirs. For example, the Hellisheidi field of Iceland, which is the site of the CarbFix project (Gislason et al., 2010; Matter et al., 2016), has a 2-km-deep record of natural carbonation, with up to ~100 kg m^{-3} CO_2 down to ~800 m depth and little carbonation below (Wiese et al., 2008). With the composition of the Icelandic basalt (8 wt% MgO and 11 wt% CaO (Alfredsson et al., 2013)) and the maximum degree of reaction of 50%, it could store up to ~260 kg m^{-3} CO_2 at all depths because the Icelandic upper crust has the porosity of ~10% down to ~2 km (Jonsson and Stefansson, 1982). The difference between the storage potential and the actual degree of carbonation, even after the period of 70,000 to 400,000 years (Franzson et al., 2005), may be explained by multiple factors, such as the availability of carbon in natural water, the efficiency of hydrothermal circulation, low reaction rates, the consumption of divalent cations with hydration, and the armoring of reactive surface. The success of the CarbFix and CarbFix2 projects (>95% and >50%, respectively, of injected CO_2 were fixed as carbonated minerals (Matter et al., 2016; Gunnarsson et al., 2018; Snaebjornsdottir et al., 2020)) suggests that the observed degree of natural carbonation is not the upper bound, and approaching the full storage potential may be possible by optimizing injection strategy and fluid chemistry. The confining pressure presents inescapable constraints on in-situ mineral carbonation, but the maximum degree of reaction, as predicted by our theory, could serve as an ideal that motivates various engineering solutions.

CRediT authorship contribution statement

Jun Korenaga: Writing – original draft, Methodology, Investigation, Funding acquisition, Formal analysis, Conceptualization.

Declaration of competing interest

The authors declare that they have no known competing financial interests or personal relationships that could have appeared to influence the work reported in this paper.

Acknowledgements

This material is based upon work supported by Yale Center for Nature Carbon Capture. The author thanks Dave Bercovici, Peter Kelemen, and Mike Oristaglio for constructive discussion. This manuscript also benefited from careful official reviews by Benjamin Tutolo.

Data availability

No data was used for the research described in the article.

References

Alfredsson, H.A., Oelkers, E.H., Hardarsson, B.S., Franzson, H., Gunnlaugsson, E., Gislason, S.R., 2013. The geology and water chemistry of the Hellisheidi, SW-Iceland carbon storage site. Int. J. Greenh. Gas Control 12, 399–418.

Audigane, P., Royer, J.-J., Kaieda, H., 2002. Permeability characterization of the Soultz and Ogachi large-scale reservoir using induced microseismicity. Geophysics 67, 204–211.

Bielicki, J.M., Pollak, M.F., Fitts, J.P., Peters, C.A., Wilson, E.J., 2014. Causes and financial consequences of geologic CO_2 storage reservoir leakage and interference with other subsurface resources. Int. J. Greenh. Gas Control 20, 272–284.

Cai, M., 2010. Practical estimates of tensile strength and Hoek-Brown strength parameter m_i of brittle rocks. Rock Mech. Rock Eng. 43, 167–184.

Dullien, F.A.L., 1979. Porous Media: Fluid Transport and Pore Structure. Academic Press, New York.

Escartin, J., Hirth, G., Evans, B., 2001. Strength of slightly serpentinized peridotites: implications for the tectonics of oceanic lithosphere. Geol. Soc. Am. Bull. 29 (11), 1023–1026.

Evans, O., Spiegelman, M., Kelemen, P.B., 2020. Phase-field modeling of reaction-driven cracking: determining conditions for extensive olivine serpentinization. J. Geophys. Res., Solid Earth 125, e2019JB018614. https://doi.org/10.1029/2019JB018614.

Fletcher, R.C., Buss, H.L., Brantley, S.L., 2006. A spheroidal weathering model coupling porewater chemistry to soil thicknesses during steady-state denudation. Earth Planet. Sci. Lett. 244, 444–457.

Franzson, H., Kristjansson, B.R., Gunnarsson, G., Björnsson, G., Hjartarson, A., Steingrimsson, B., Gunnlaugsson, E., Gislason, G., 2005. The Hengill-Hellisheidi geothermal field. Development of a conceptual geothermal model. In: Proceeds World Geothermal Congress, pp. 1–7.

Gale, A., Dalton, C.A., Langmuir, C.H., Su, Y., Schilling, J.-G., 2013. The mean composition of ocean ridge basalts. Geochem. Geophys. Geosyst. 14. https://doi.org/10.1029/2012GC004334.

Gislason, S.R., Wolff-Boenisch, D., Stefansson, A., Oelkers, E.H., Gunnlaugsson, E., Sigurdardottir, H., Sigfusson, B., Broecker, W.S., Matter, J.M., Stute, M., Axelsson, G., Fridriksson, T., 2010. Mineral sequestration of carbon dioxide in basalt: a pre-injection overview of the CarbFix project. Int. J. Greenh. Gas Control 4, 537–545.

Goldberg, D.S., Takahashi, T., Slagle, A.L., 2008. Carbon dioxide sequestration in deep-sea basalt. Proc. Natl. Acad. Sci. USA 105, 9920–9925.

Gunnarsson, I., Aradottir, E.S., Oelkers, E.H., Clark, D.E., Arnarson, M.P., Sigfusson, B., Snaebjornsdottir, S.O., Matter, J.M., Stute, M., Juliusson, B.M., Gislason, S.R., 2018. The rapid and cost-effective capture and subsurface mineral storage of carbon and sulfur at the CarbFix2 site. Int. J. Greenh. Gas Control 79, 117–126.

Heap, M.J., Wadsworth, F.B., Heng, Z., Xu, T., Griffiths, L., Velasco, A.A., Vaire, E., Vistour, M., Reuschle, T., Troll, V.R., Deegan, F.M., Tang, C., 2021. The tensile strength of volcanic rocks: experiments and models. J. Volcanol. Geotherm. Res. 418, 107348.

Hyndman, R.D., Peacock, S.M., 2003. Serpentinization of the forearc mantle. Earth Planet. Sci. Lett. 212, 417–432.

Jackson, M.D., Heap, M.J., Vola, G., Ardit, M., Rhodes, J.M., Peterson, J.G., Tamura, N., Gudmundsson, M.T., 2024. Material and mechanical properties of young basalt in drill cores from the oceanic island of Surtsey, Iceland. Geol. Soc. Am. Bull. 136. https://doi.org/10.1130/B37037.1.

Jamtveit, B., Malthe-Sorenssen, A., Kostenko, O., 2008. Reaction enhanced permeability during retrogressive metamorphism. Earth Planet. Sci. Lett. 267, 620–627.

Jonsson, G., Stefansson, V., 1982. Density and porosity logging in the IRDP hole, Iceland. J. Geophys. Res. 87, 6619–6630.

Kelemen, P.B., Aines, R., Bennett, E., Benson, S.M., Carter, E., Coggon, J.A., de Obeso, J.C., Evans, O., Gadikota, G., Dipple, G.M., Godard, M., Harris, M., Higgins, J.A., Johnson, K.T.M., Kourim, F., Lafay, R., Lambart, S., Manning, C.E., Matter, J.M., Michibayashi, K., Morishita, T., Noël, J., Okazaki, K., Renforth, P., Robinson, B., Savage, H., Skarbek, R., Speigelman, M.W., Takazawa, E., Teagle, D., Urai, J.L., Wilcox, J., the Oman Drilling Project Phase 1 Scientific Party, 2018. *In situ* carbon mineralization in ultramafic rocks: natural processes and possible engineered methods. Energy Proc. 146, 92–102.

Kelemen, P.B., Hirth, G., 2012. Reaction-driven cracking during retrograde metamorphism: olivine hydration and carbonation. Earth Planet. Sci. Lett. 345–348, 81–89.

Kelemen, P.B., Matter, J., 2008. In situ carbonation of peridotite for CO_2 storage. Proc. Natl. Acad. Sci. USA 105, 17295–17300.

Kelemen, P.B., Matter, J., Streit, E.E., Rudge, J.F., Curry, W.B., Blusztajn, J., 2011. Rates and mechanisms of mineral carbonation in peridotite: natural processes and recipes for enhanced, in situ CO_2 capture and storage. Annu. Rev. Earth Planet. Sci. 39, 545–576.

Lambert, S., Savage, H.M., Robinson, B.G., Kelemen, P.B., 2018. Experimental investigation of the pressure of crystallization of $Ca(OH)_2$: implications for the reactive cracking process. Geochem. Geophys. Geosyst. 19, 3448–3458. https://doi.org/10.1029/2018GC007609.

Li, L., Kohler, F., Dziadkowiec, J., Royne, A., Espinosa Marzal, R.M., Bresme, F., Jettestuen, E., Dysthe, D.K., 2022. Limits to crystallization pressure. Langmuir 38, 11265–11273.

Lippard, S.J., Shelton, A.W., Gass, I., 1986. The Ophiolite of Northern Oman. Blackwell, Oxford, melt1.

Lockner, D.A., 1995. Rock failure. In: Rock Physics and Phase Relations. AGU, pp. 127–147.

Marieni, C., Henstock, T.J., Teagle, D.A.H., 2013. Geological storage of CO_2 within the oceanic crust by gravitational trapping. Geophys. Res. Lett. 40, 6219–6224.

Matter, J.M., Stute, M., Snaebjornsdottir, S.O., Oelkers, E.H., Gislason, S.R., Aradottir, E.S., Sigfusson, B., Gunnarsson, I., Sigurdardottir, H., Gunnlaugsson, E., Axelsson, G., Alfredsson, H.A., Wolff-Boenisch, D., Mesfin, K., Fernandez de la Reguera Taya, D., Hall, J., Dideriksen, K., Broecker, W.S., 2016. Rapid carbon mineralization for permanent disposal of anthropogenic carbon dioxide emissions. Science 352, 1312–1314.

McGrail, B.P., Schaef, H.T., Ho, A.M., Chien, Y.-J., Dooley, J.J., Davidson, C.L., 2006. Potential for carbon dioxide sequestration in flood basalts. J. Geophys. Res. 111, B12201. https://doi.org/10.1029/2005JB004169.

Moore, D.E., Lockner, D.A., 2004. Crystallographic controls on the frictional behavior of dry and water-saturated sheet structure minerals. J. Geophys. Res. 109, B03401. https://doi.org/10.1029/2003JB002582.

Moore, D.E., Lockner, D.A., 2007. Comparative deformation behavior of minerals in serpentinized ultramafic rock: application to the slab-mantle interface in subduction zones. Int. Geol. Rev. 49, 401–415.

Mura, T., 1987. Micromechanics of Defects in Solids, 2nd ed. Kluwer Academic.

Nagurney, A., Lahiri, N., Murchland, M., Blondes, M.S., Thakurta, J., Gadikota, G., Schaef, T., 2023. Carbon-negative mining advancements to promote the green energy transition. In: AGU Fall Meeting, pp. V22A–07.

National Academies of Sciences, Engineering, and Medicine, 2019. Negative Emissions Technologies and Reliable Sequestration: A Research Agenda. National Academy Press.

Paterson, M.S., Wong, T.-F., 2005. Experimental Rock Deformation — The Brittle Field. Springer.

Perras, M.A., Diederichs, M.S., 2014. A review of the tensile strength of rock: concepts and testing. Geotech. Geolog. Eng. 32, 525–546.

Rochelle, C.A., Czernichowski-Lauriol, I., Milodowski, A.E., 2024. The impact of chemical reactions on CO_2 storage in geological formations: a brief review. In: Baines, S.J., Worden, R.H. (Eds.), Geological Storage of Carbon Dioxide, vol. 233. Geol. Soc. London, pp. 87–106.

Røyne, A., Jamtveit, B., 2015. Pore-scale controls on reaction-driven fracturing. Rev. Mineral. Geochem. 80, 25–44.

Rudge, J.F., Kelemen, P.B., Spiegelman, M., 2010. A simple model of reaction-induced cracking applied to serpentinization and carbonation of peridotite. Earth Planet. Sci. Lett. 291, 215–227.

Scherer, G.W., 1999. Crystallization in pores. Cem. Concr. Res. 29, 1347–1358.

Scholz, C.H., 2019. The Mechanics of Earthquakes and Faulting, 3rd ed. Cambridge Univ. Press.

Snaebjornsdottir, S.O., Sigfusson, B., Marieni, C., Goldberg, D., Gislason, S.R., Oelkers, H.E., 2020. Carbon dioxide storage through mineral carbonation. Nature Rev. Earth Environ. 1, 90–102.

Snaebjornsdottir, S.O., Wiese, F., Fridriksson, T., Armannsson, H., Einarsson, G.M., Gislason, S.R., 2014. CO_2 storage potential of basaltic rocks in Iceland and the oceanic ridges. Energy Proc. 63, 4585–4600.

Steiger, M., 2005. Crystal growth in porous materials, I, the crystallization pressure of large crystals. J. Cryst. Growth 282, 455–469.

Thibeau, S., Bachu, S., Birkholzer, J., Holloway, S., Neele, F., Zhau, Q., 2014. Using pressure and volumetric approaches to estimate CO_2 storage capacity in deep saline aquifers. Energy Proc. 63, 5294–5304.

Ulven, O.I., Jamtveit, B., Malthe-Sorenssen, A., 2014. Reaction-driven fracturing of porous rock. J. Geophys. Res., Solid Earth 119, 7473–7486. https://doi.org/10.1002/2014JB011102.

Uno, M., Koyanagawa, K., Kasahara, H., Okamoto, A., Tsuchiya, N., 2022. Volatile-consuming reactions fracture rocks and self-accelerate fluid flow in the lithosphere. Proc. Natl. Acad. Sci. USA 119, e2110776118. https://doi.org/10.1073/pnas.2110776118.

Wiese, F., Fridriksson, T., Armannsson, H., 2008. CO_2 fixation by calcite in high-temperature geothermal systems in Iceland. Tech. Rep. 2008/003, ISOR.

Wilson, E.J., Johnson, T.L., Keith, D.W., 2003. Regulating the ultimate sink: managing the risks of geologic CO_2 storage. Environ. Sci. Technol. 37, 3476–3483.

Wolterbeek, T.K.T., van Noort, R., Spiers, C.J., 2018. Reaction-driven casing expansion: potential for wellbore leakage mitigation. Acta Geotech. 13, 341–366.

Zheng, X., Cordonnier, B., Zhu, W., Renard, F., Jamtveit, B., 2018. Effects of confinement on reaction-induced fracturing during hydration of periclase. Geochem. Geophys. Geosyst. 19, 2661–2672. https://doi.org/10.1029/2017GC007322.

Zhou, Q., Birkholzer, J.T., Tsang, C.-F., Rutqvist, J., 2008. A method for quick assessment of CO_2 storage capacity in closed and semi-closed saline formations. Int. J. Greenh. Gas Control 2, 626–639.

Zhu, W., Fusseis, F., Lisabeth, H., Xing, T., Xiao, X., De Andrade, V., Karato, S., 2016. Experimental evidence of reaction-induced fracturing during olivine carbonation. Geophys. Res. Lett. 43, 9535–9543. https://doi.org/10.1002/2016GL070834.

Zoback, M.D., Gorelick, S.M., 2012. Earthquake triggering and large-scale geologic storage of carbon dioxide. Proc. Natl. Acad. Sci. USA 109, 10164–10168.